

---

# LightMoE: Reducing Mixture-of-Experts Redundancy through Expert Replacing

---

Jiawei Hao<sup>1</sup> Zhiwei Hao<sup>2</sup> Jianyuan Guo<sup>2</sup> Li Shen<sup>3</sup> Yong Luo<sup>4</sup> Han Hu<sup>1</sup> Dan Zeng<sup>5</sup>

## Abstract

Mixture-of-Experts (MoE) based Large Language Models (LLMs) have demonstrated impressive performance and computational efficiency. However, their deployment is often constrained by substantial memory demands, primarily due to the need to load numerous expert modules. While existing expert compression techniques like pruning or merging attempt to mitigate this, they often suffer from irreversible knowledge loss or high training overhead. In this paper, we propose a novel expert compression paradigm termed expert replacing, which replaces redundant experts with parameter-efficient modules and recovers their capabilities with low training costs. We find that even a straightforward baseline of this paradigm yields promising performance. Building on this foundation, we introduce LightMoE, a framework that enhances the paradigm by introducing adaptive expert selection, hierarchical expert construction, and an annealed recovery strategy. Experimental results show that LightMoE matches the performance of LoRA fine-tuning at a 30% compression ratio. Even under a more aggressive 50% compression rate, it outperforms existing methods and achieves average performance improvements of 5.6% across five diverse tasks. These findings demonstrate that LightMoE strikes a superior balance among memory efficiency, training efficiency, and model performance.

## 1. Introduction

LLMs leveraging Sparse Mixture-of-Experts (MoE) architectures, exemplified by models such as DeepSeek-MoE (Dai et al., 2024; Liu et al., 2024a) and OLMoE (Muenighoff et al., 2025), have recently received significant attention. Their design offers excellent performance and notable efficiency in both training and inference processes. However, a primary challenge associated with these powerful models is their substantial memory footprint. Loading numerous expert modules demands considerable memory resources, which constrains their practical applicability and impedes widespread deployment in real-world scenarios. While expert offloading techniques (Kim et al., 2024; Eliseev & Mazur, 2023; Yu et al., 2025) mitigate GPU memory limits, they introduce prohibitive inference latency due to the frequent transfer of weights from CPU memory or disk. Consequently, direct parameter compression has become a critical research frontier.

Current MoE compression methods largely follow two paradigms: expert pruning (Lu et al., 2024; Yang et al., 2024c) and expert merging (Li et al., 2024b; Liu et al., 2024c; Chen et al., 2025a). Expert pruning methods, such as MoE-Pruner, which prunes weights based on activation frequencies and router importance scores, aim to remove less critical experts. However, a significant drawback of pruning is the irreversible loss of pruned expert knowledge, which results in substantial performance degradation. On the other hand, expert merging seeks to combine multiple experts into a single, more compact representation. However, merging experts inherently diminishes the model’s representational diversity, and determining an optimal merging strategy remains a significant challenge in the field. Despite these challenges, recent findings (Liu et al., 2024b; Lu et al., 2024) reveal that current MoEs contain significant parameter redundancy. Some studies (Wang et al., 2024) also indicate a high concentration of active experts in fine-grained MoE models when applied to specific tasks.

Based on these challenges and observations, we explore a straightforward solution: *Can we simply replace less critical experts with parameter-efficient modules and subsequently recover their capabilities with low-cost training?* This idea raises three fundamental questions: (1) *expert selection:*

---

<sup>1</sup>School of Information and Electronics, Beijing Institute of Technology, Beijing, China <sup>2</sup>Department of Computer Science, City University of Hong Kong, Hong Kong, China <sup>3</sup>Shenzhen Campus of Sun Yat-sen University, Shenzhen, China <sup>4</sup>School of Computer Science, Wuhan University, Wuhan, China <sup>5</sup>School of Communication and Information Engineering, Shanghai University, Shanghai, China. Correspondence to: Han Hu <hhu@bit.edu.cn>.

How to select the less important experts for replacement? (2) *module construction*: How to design and initialize the parameter-efficient modules? (3) *efficient recovery*: How to restore model performance with minimal training overhead? A simple way to materialize this idea is to replace these less frequently activated experts with Low-Rank Adaptation (LoRA) (Hu et al., 2022), and subsequently fine-tune the modified model. As illustrated in Figure 1, this directly replacing strategy achieves performance comparable to the existing method MC-SMoE (Li et al., 2024b). However, both approaches suffer from significant performance degradation, particularly at higher compression ratios. This suggests that even experts deemed “inactive” or less critical for a specific task may still harbor fundamental abilities and knowledge crucial for overall model capabilities. Attempting to restore this lost knowledge and alleviate performance degradation solely through fine-tuning proves to be a difficult endeavor.

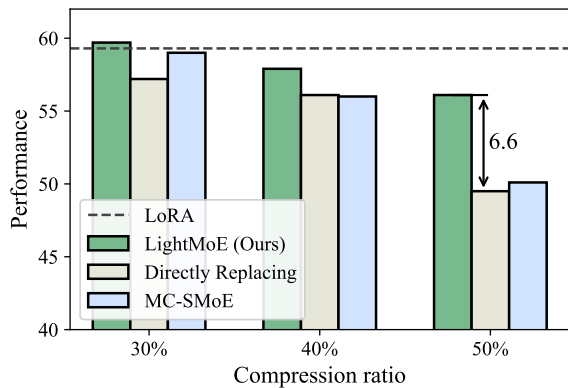


Figure 1. Performance comparison across different compression ratios on the Math task. While the directly replacing strategy performs comparably to MC-SMoE, both suffer from significant performance degradation, particularly at higher compression ratios

In this work, we propose LightMoE, a framework for compressing redundant experts in MoE models via expert replacing. The framework comprises three key stages: selecting less important experts through adaptive thresholding, constructing hierarchical experts, and progressively replacing the original experts through annealing. First, LightMoE calculates the relative importance of experts within and across layers to establish an adaptive threshold. This threshold serves as a dynamic criterion to select less critical experts. Next, the selected experts are grouped and replaced with a smaller number of shared bases, each equipped with task-specific low-rank adaptation parameters to preserve specialization. Finally, during the fine-tuning phase, the original experts are gradually annealed into their corresponding shared bases, allowing the model to adapt smoothly to the compressed structure. Experimental results across five diverse tasks show that LightMoE achieves performance comparable to LoRA fine-tuning at a 30% compression ratio. Even under a more aggressive 50% compression rate with the

same training budget, it delivers average performance improvements of 5.6% and 3.8% over existing methods and the directly replacing baseline, respectively.

## 2. Related Works

### 2.1. Mixture-of-Experts LLMs

In contrast to traditional dense Large Language Models (LLMs) such as the LLaMA series (Touvron et al., 2023; Grattafiori et al., 2024), Mixture of Experts (MoE) architectures offer a compelling approach to expanding model capacity while reducing training and inference costs. The majority of existing MoE (Lepikhin et al., 2020; Dai et al., 2022; Shen et al., 2024) implementations employ coarse-grained architectures with relatively few experts. For instance, the Mixtral series (Jiang et al., 2024) activate only 2 out of 8 available experts during computation. This limitation necessitates that each expert must handle diverse patterns across multiple domains simultaneously.

More recently, fine-grained expert segmentation (Dai et al., 2024; Yang et al., 2024a;b) has gained significant attention, as it enables a greater variety of expert combinations and demonstrates superior performance. In the OLMoE (Muenighoff et al., 2025), there are as many as 64 experts, with 8 active experts. However, these fine-grained MoE architectures inherit substantial memory footprints from storing all expert weights. Interestingly, recent studies (Wang et al., 2024) reveal that this fine-grained division ensures a high degree of specialization among the experts. We argue that this distinct specialization presents opportunities for task-specific model compression, enabling more efficient deployment for downstream applications.

### 2.2. MoE Compression Methods

Given that experts constitute a significant portion of memory requirements, prior work on MoE model efficiency can be categorized into these principal approaches: expert off-loading (Kim et al., 2024; Eliseev & Mazur, 2023; Yu et al., 2025), expert compression (Lu et al., 2024; Yang et al., 2024c; Li et al., 2024b; Liu et al., 2024c), and more general compression strategies such as quantization (Li et al., 2024a; Huang et al., 2024) and knowledge distillation (Xu et al., 2024; Kim et al., 2025).

In this work, we focus on the expert compression technique, which can be broadly categorized into expert pruning (Lu et al., 2024; Yang et al., 2024c) and expert merging (Li et al., 2024b; Liu et al., 2024c; Chen et al., 2025a). Expert pruning methods focus on pruning dense matrices and removing redundant experts. For instance, MoE-Pruner (Xie et al., 2024) prunes weights based on activation frequencies, while NAAE (Lu et al., 2024) searches for expert combinations that minimize output deviation. However, these approaches

often lead to substantial performance degradation due to the permanent loss of expert knowledge. Furthermore, search-based methods like NAEF are ill-suited for fine-grained MoE architectures due to combinatorial explosion. In the case of OLMoE with 64 experts, a 50% reduction results in an overwhelming search space of  $C(64, 32) \approx 1.8 \times 10^{18}$  combinations per layer. Expert merging methods aim to consolidate multiple experts into fewer ones. For example, MC-SMoE (Li et al., 2024b) clusters experts according to their routing statistics and subsequently merges each cluster into a single representative expert. However, this approach inherently diminishes the model’s representational diversity, and identifying an optimal merging strategy is non-trivial. Furthermore, while MC-SMoE employs progressive low-rank decomposition during retraining for further expert compression, it introduces substantial training overhead. This is because the decomposition process requires computing gradients from the original experts. Recent efforts have also explored dynamic inference optimization. Specifically, He et al. (2025) propose replacing auxiliary activated experts with compressed modules to reduce active parameters. While this effectively lowers inference computational costs, it does not address the substantial memory footprint stemming from the total parameters, as the non-active experts still require storage.

Distinct from the aforementioned approaches, we propose a novel expert compression paradigm termed *expert replacing*. Empirical results show that even a simple baseline of this paradigm achieves performance comparable to, or slightly superior to, existing methods. Building on this foundation, we further propose optimizations across three key dimensions: expert selection, module construction, and efficient recovery. This design not only enables effective model compression but also preserves the specialized capability of the model with minimal overhead. Consequently, it strikes an optimal balance among memory efficiency, training efficiency, and model performance. From a broader perspective, expert merging can be viewed as a special case of our expert replacing paradigm. Fundamentally, merging does not reduce the number of experts indexed by the router, but instead maps multiple indices to the same parameters. In essence, this is equivalent to replacing multiple original experts with a single shared expert.

### 2.3. Low-Rank Adaptation

The immense complexity and computational demands of LLMs with billions of parameters pose substantial challenges for their adaptation to specific downstream tasks. Parameter-efficient fine-tuning (PEFT) (Xu et al., 2023; Han et al., 2024) aims to minimize the fine-tuning parameters while achieving performance comparable to full fine-tuning. Typical PEFT methods include adapter (Rücklé et al., 2021; Lei et al., 2023; Wang et al., 2022), soft prompt (Li & Liang,

2021; Lester et al., 2021; Wang et al., 2023b), and low-rank adaptation (Hu et al., 2022; Meng et al., 2024; Liu et al., 2024d; Wu et al., 2024; Hayou et al., 2024). LoRA (Hu et al., 2022) decomposes the original weight matrices into low-rank components. Inspired by this, we propose replacing multiple experts with parameter-efficient modules, which effectively reduce the number of expert parameters while preserving the diversity of the experts. Moreover, our approach incurs significantly lower training overhead compared to full fine-tuning the entire compressed model.

## 3. Method

In a MoE layer, a router module selects one or more experts to process each input based on its routing decision, and the outputs of the selected experts are aggregated to form the output. To enable redundant expert compression, the proposed LightMoE framework first measures the importance of each expert and selects less critical candidates for compression (Section 3.1). These candidate experts are then grouped, and each group is assigned a shared base equipped with low-rank adaptation parameters to retain the specialization of the original experts (Section 3.2). Finally, during training, the original candidates are gradually replaced with their corresponding shared bases through an annealed replacement strategy (Section 3.3). Figure 2 provides an overview of the proposed framework.

### 3.1. Adaptive Expert Selection

In MoE models, redundancy manifests in two dimensions: intra-layer imbalance, where some experts contribute significantly less than others, and inter-layer variability, where different layers exhibit varying degrees of impact on model performance. Building on these observations, we define expert importance based on activation frequency and propose an adaptive strategy to select redundant experts. Specifically, this process involves two steps: computing the importance score for each expert, and identifying less important experts in each layer using an adaptive threshold that incorporates both expert-level and layer-level importance.

**Importance scoring.** A typical MoE layer comprises multiple feed-forward network experts and a routing mechanism that dynamically selects the active experts for each input token. The output of the MoE layer is computed as:

$$y = \sum_{i=1}^N G(x)_i E_i(x), \quad (1)$$

where  $x$  and  $y$  denote the input and output of the MoE layer, respectively,  $N$  is the total number of experts,  $E_i$  represents the  $i$ -th expert, and  $G(x)_i$  is the gating value assigned to expert  $i$ , indicating its relevance to the input token  $x$ .

To quantify the importance of each expert, we sample a

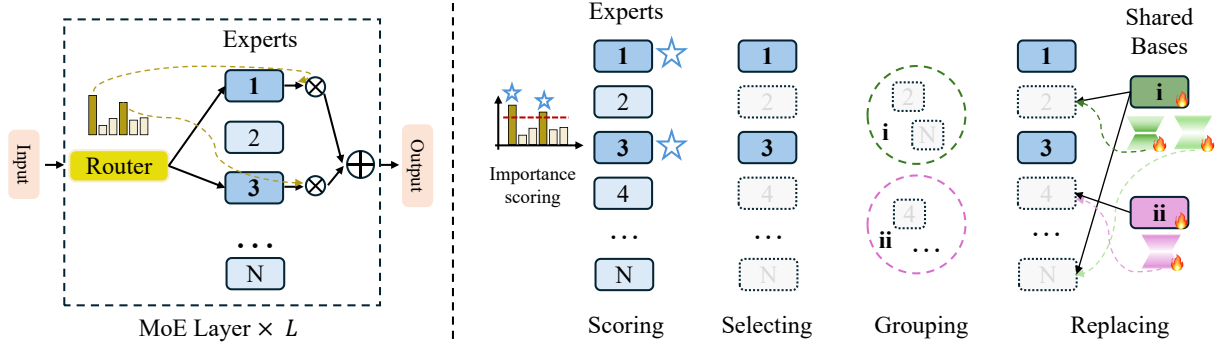


Figure 2. Overview of the proposed LightMoE framework. (Left) A standard MoE layer. (Right) The LightMoE workflow, comprising three key steps: (1) scoring experts and selecting those with lower scores as compression candidates, (2) grouping the selected candidates, and (3) replacing each group with a shared base augmented with lightweight, expert-specific adaptation parameters.

subset of the training data and aggregate gate values across all tokens. This provides a data-driven estimate of each expert’s contribution. To normalize these contributions and enable comparison across experts, we define the normalized gate score for expert  $i$  as:

$$G_i = \frac{\sum_{x \in \mathcal{X}} G(x)_i}{\sum_{i=1}^N \sum_{x \in \mathcal{X}} G(x)_i}, \quad (2)$$

where  $\mathcal{X}$  denotes the evaluation subset. This score reflects the relative importance of each expert based on its cumulative gate activation across the sampled data.

In our preliminary experiment, we used samples from the training set, totaling  $2^{17}$  tokens, to evaluate expert importance. The MoE model used is OLMoE-1B-7B-SFT (Muenighoff et al., 2025). Figure 3a presents the sorted importance scores of experts in the selected layers. The non-uniform distribution of scores confirms the existence of differences in expert importance, supporting the compression of less important experts in our proposed method.

**Adaptive thresholding.** The importance scoring results reveal that experts within the same layer exhibit varying degrees of significance. This suggests that less important experts can be compressed without substantial performance degradation. A direct approach might apply a fixed compression ratio across all experts. However, such a coarse strategy risks unnecessary performance loss.

Motivated by the observed variation in importance among experts within a layer, we hypothesize that similar differences exist across layers in MoE models. To test this, we evaluate the average output norms of router at each layer using a subset of training samples. The underlying intuition is that more important layers tend to produce stronger activations, which reflected in larger output norms. Similar ideas have also been adopted in prior studies (Song et al., 2024). Figure 3b presents the results, which show that as the model

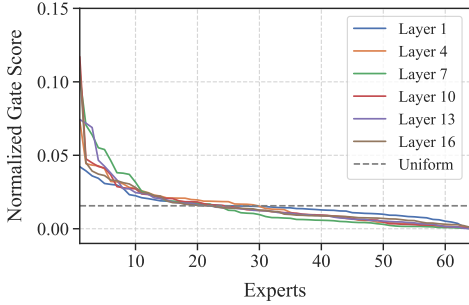
depth increases, the average router norm also rises, suggesting that deeper layers play a more critical role. Building on this insight, we propose a compression strategy that varies across layers, where shallower layers are assigned higher compression ratios, while deeper layers are preserved more conservatively. Specifically, based on the previously defined normalized gating scores, we sort experts in ascending order and select the top subset whose cumulative score just exceeds a layer-specific compression threshold. This subset is treated as less important and subject to compression. Formally, given a base threshold  $\hat{p}$ , we define the threshold for the  $j$ -th layer as:

$$\hat{p}_j = \text{clip} \left( \hat{p} \cdot e^{-\alpha(\text{norm}_j - 1)}, p_{\min}, p_{\max} \right), \quad (3)$$

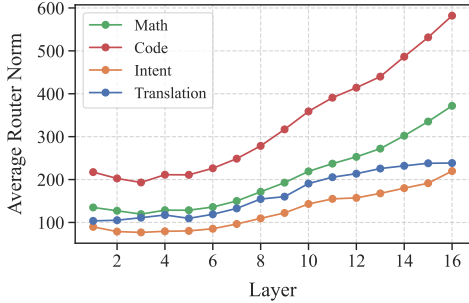
where  $\text{norm}_j$  is the ratio of the norm of layer  $j$  to the average norm across all layers. Thus, if the norm of layer  $j$  exceeds the mean, the exponential term drives  $\hat{p}_j$  below the base threshold  $\hat{p}$ .  $\alpha$  is an exponential decay coefficient that modulates the strength of the adjustment; we set  $\alpha = 0.3$  in all experiments.  $\text{clip}(p, p_{\min}, p_{\max})$  truncates the adjusted threshold to lie within  $[p_{\min}, p_{\max}]$  for numerical stability. In our experiments we set  $p_{\min} = 0.8\hat{p}$  and  $p_{\max} = 1.2\hat{p}$ . This adaptive thresholding mechanism allows the proposed method to account for both intra-layer and inter-layer variations in expert importance, resulting in a more effective compression approach.

### 3.2. Hierarchical Expert Construction

After selecting less important experts in each layer, we aim to compress them to reduce memory consumption. However, directly removing or merging them may lead to a loss of expert-specific knowledge. To solve this, we propose a hierarchical expert representation that decomposes each expert into a shared base and a expert-specific low-rank adapter. This design allows the model to capture common patterns via the shared base while preserving specific ca-



(a) Sorted expert-wise normalized gate scores. Experts exhibit varying importance across layers, highlighting *intra-layer* differences in specialization.



(b) Average output norms of router per layer. The increasing norm with depth suggests growing *inter-layer* importance in deeper layers.

Figure 3. Analysis of expert importance in OLMoE-1B-7B-SFT.

pabilities through efficient parameterization. Specifically, let  $N'$  denote the number of experts to be compressed in a given layer, where each expert is parameterized by a weight matrix  $W_1, W_2, \dots, W_{N'} \in \mathbb{R}^{n \times m}$ . We first construct the shared base  $W_{\text{share}}$  as the weighted average of these experts, utilizing their normalized gate scores  $G_i$  as weights<sup>1</sup>:

$$W_{\text{share}} = \frac{\sum_{i=1}^{N'} G_i W_i}{\sum_{i=1}^{N'} G_i}. \quad (4)$$

Subsequently, each original expert  $W_{n'}$  is reconstructed hierarchically as  $W_{\text{share}} + B_{n'} A_{n'}$ , where  $B_{n'} \in \mathbb{R}^{n \times r}$  and  $A_{n'} \in \mathbb{R}^{r \times m}$  represent the expert-specific low-rank adaptation terms, with  $r \ll \min(n, m)$ .

While a single shared base can serve as a common foundation, it may not adequately capture the diverse knowledge embedded across multiple less important experts. To address this, we extend the framework to support multiple shared bases. Suppose we choose to use  $M$  shared bases, where  $M < N'$ . The  $N'$  experts are partitioned into  $M$  groups, each represented by a shared base. Following the

<sup>1</sup>For simplicity, we represent each expert using a single weight matrix. In practice, all parameter matrices in each expert are processed in the same manner.

approach in (Li et al., 2024b), we select the top  $M$  experts with the highest normalized gate scores  $G_i$  as dominant experts. Each remaining expert is then assigned to the dominant expert with which it shares the highest semantic similarity. This similarity is computed as the average sample-wise cosine similarity between the routing logits of the non-dominant and dominant experts, using the same evaluation samples from the scoring phase. Once grouped, each set of experts is compressed into a shared base following the weighted average procedure described above.

**Expert-Level Compression Ratio.** Under the proposed scheme, multiple full-rank experts are represented using a smaller number of full-rank shared bases, each augmented with several low-rank adaptation terms. The resulting expert compression ratio  $\rho$  is given by:

$$\rho = 1 - \frac{(N - N' + M)nm + N'r(n + m)}{N \cdot nm}. \quad (5)$$

Since  $M < N'$  and  $r \ll \min(n, m)$ , this strategy leads to a substantial reduction in parameter count while preserving model capacity and diversity.

### 3.3. Annealed Expert Replacement

Directly replacing the original experts with shared bases and low-rank adaptation parameters can lead to significant performance degradation due to the abrupt change in the model parameter space. To mitigate this, we introduce an annealed expert replacement strategy, which gradually transitions each expert from its original form to its compressed representation during fine-tuning. This smooth transition helps preserve performance by maintaining continuity in the optimization trajectory. A detailed empirical analysis of the training dynamics is provided in appendices (Section C).

Concretely, consider a less important expert  $W_{n'}$  selected for compression. During fine-tuning, its effective parameter matrix  $W_{n'}^*$  is computed as a weighted combination of three components: the original expert  $W_{n'}$ , the shared base  $W_{\text{share}}$ , and the expert-specific low-rank adaptation term  $B_{n'} A_{n'}$ . The combined parameter is given by:

$$W_{n'}^* = \beta W_{n'} + (1 - \beta) W_{\text{share}} + B_{n'} A_{n'}, \quad (6)$$

where  $\beta \in [0, 1]$  is an annealing factor that is gradually decays from 1 to 0 over the course of fine-tuning. At the beginning of training,  $\beta = 1$ , so the model behaves identically to the original MoE. As training progresses and  $\beta$  decays, the model incrementally shifts towards using the compressed representation. This progressive interpolation ensures a smooth adaptation to the shared and low-rank parameter space. At the end of fine-tuning,  $\beta = 0$ , and the original expert parameters  $W_{n'}$  are no longer used. They can thus be safely removed during inference, reducing the model size and achieving the desired compression. We

utilize a simple yet effective decay strategy for  $\beta$ :

$$\beta = \max\left(1 - \frac{t}{\epsilon T}, 0\right), \quad (7)$$

where  $T$  is the total steps of training and  $t$  is the current step. The parameter  $\epsilon \in [0, 1]$  is the end ratio that controls when  $\beta$  completely decays to 0. For instance, when  $\epsilon = 0.4$ ,  $\beta$  reaches zero at  $t = 0.4T$ . When  $\epsilon = 0$ ,  $\beta$  is set to zero at the beginning of training, which means directly replacing the original experts with the parameter-efficient modules without any annealing period.

## 4. Experiments

### 4.1. Experiment Setup

**Datasets and evaluation.** Following ESFT (Wang et al., 2024), we evaluate our LightMoE method in two LLM customization scenarios: (1) preserving **specific ability in a domain** in which the model already demonstrates reasonable performance, and (2) adapting the model to a **narrow but unfamiliar specialized task** while achieving compression. For preservation, we target Math, Coding, and Commonsense Reasoning domains. For the Math domain, we train on MetaMathQA (Yu et al., 2024) and evaluate using GSM8K (Cobbe et al., 2021). For the Code domain, we use CodeFeedback (Zheng et al., 2024) for training and HumanEval (Chen et al., 2021) for evaluation. Evaluation protocols are consistent with those used in existing works (Muennighoff et al., 2025; Ivison et al., 2023; Wang et al., 2023a). For the Commonsense Reasoning domain, we utilize the Cleaned Alpaca Dataset (Taori et al., 2023) for training. Following standard evaluation protocols (Taori et al., 2023; Liu et al., 2024d), we report the averaged accuracy on eight representative commonsense reasoning tasks, such as ARC (Clark et al., 2018), BoolQ (Clark et al., 2019), PIQA (Bisk et al., 2020), and WinoGrande (Sakaguchi et al., 2021). For adaptation, we focus on intent recognition and low-resource translation. The intent recognition task comes from the BDCI-21 Smart HCI NLU Challenge.<sup>2</sup> The low-resource translation task utilizes the ChrEn dataset (Zhang et al., 2020), which requires translating Cherokee into English. In line with ESFT (Wang et al., 2024), during evaluation, we compute the exact match rate between model predictions and reference answers on intent recognition task. For the translation task, we use GPT-4 to assign a score between 0 and 10 according to output quality relative to the reference.<sup>3</sup>

**Backbone model.** We use OLMoE-1B-7B-SFT (Muennighoff et al., 2025) with 6.9B total and 1.3B active parameters as the pretrained model in our experiments. The model

<sup>2</sup><https://www.datafountain.cn/competitions/511>

<sup>3</sup>The exact version used is gpt-4-1106-preview. The scores are normalized to match the scale of other reported metrics.

includes a fine-grained set of 64 experts for each MoE layer.

**Baselines.** We compare our proposals to a comprehensive set of baselines. First, we evaluate state-of-the-art expert compression methods. We adopt MC-SMoE (Li et al., 2024b) in two variants. The original version initializes by merging experts to a 30% compression ratio and employs progressive low-rank decomposition to reach 40% and 50% ratios. However, this approach requires computing gradients from original experts, leading to substantial overhead. Therefore, we also test a modified version using LoRA fine-tuning to ensure a fair computational comparison. Additionally, we include HC-SMoE (Chen et al., 2025a), which employs hierarchical clustering based on expert outputs to ensure robust merging independent of routing decisions. Furthermore, we evaluate MoBE (Chen et al., 2025b), which decomposes expert weights into shared basis matrices and expert-specific transformations. Second, due to the lack of prior work on expert replacing, we introduce two strong baselines: “Replace (w/o shared)” and “Replace (w. shared)”, which directly replace less important experts with LoRA adapters, either without adding shared base or with one shared base, respectively. Both use LoRA fine-tuning to recover performance. Finally, we include full fine-tuning and LoRA fine-tuning on the original model to benchmark the performance upper bound.

**Training details.** All methods use the AdamW optimizer (Loshchilov & Hutter, 2019) with a batch size of 32, and a learning rate of 1e-4. For our method, we adopt a low-rank of 16 for all expert parameters and set the group size to 3. The low-rank matrices are initialized following the standard strategy (Hu et al., 2022), which uses a random Gaussian initialization for  $A$  and zero for  $B$ . To ensure a fair comparison, the rank for baseline methods is adjusted to maintain an equivalent number of trainable parameters. For model preservation, we adopt a training step setting of 2000. For model adaptation, training is limited to 500 steps due to smaller datasets. The optimal end ratio  $\epsilon$  is determined by grid search from  $\{0.1, 0.2, 0.3, 0.4, 0.5\}$ .

### 4.2. Main Results

Table 1 reports the main results on five tasks at three compression ratios. Our method consistently achieves the best or second-best performance across various compression ratios. Remarkably, at a 30% compression ratio, our method performs comparably to LoRA, even surpassing it on some tasks. This suggests that replacing extremely unimportant experts with parameter-efficient modules even benefits downstream task performance. At a 50% compression ratio with the same training budget, our method significantly outperforms existing methods, achieving average performance improvements of 5.6% and 3.8% over existing methods and the directly replacing baseline, respectively. Besides, even

## LightMoE: Reducing Mixture-of-Experts Redundancy through Expert Replacing

Table 1. Main performance comparison across methods and tasks at different compression ratios. ‘\*’ indicates the full method as described in the original paper. ‘# Params’ is the number of trainable parameters. Best results are shown in **bold** and second-best results are underlined. Our method LightMoE consistently achieves good performance among all tasks under different compression settings.

Ratio	Methods	# Params	Math	Code	Commonsense	Specialized Tasks		Average
			GSM8K	HumanEval	8 Sub-Tasks	Intent	Translation	
0%	Original	-	49.3	55.0	60.6	9.8	13.6	37.7
0%	Full FT	6.92B	61.2	49.7	54.2	79.2	37.1	56.3
0%	LoRA	0.45B	59.8	54.2	61.4	73.0	29.2	55.5
30%	MoBE	0.45B	52.9	41.3	<b>58.3</b>	69.4	30.3	50.4
	HC-SMoE	0.45B	40.6	41.7	55.5	64.0	<b>32.4</b>	46.8
	MC-SMoE	0.45B	<u>59.0</u>	51.7	55.1	70.2	<u>30.9</u>	53.4
	Replace (w/o shared)	0.45B	57.2	<u>53.8</u>	55.6	69.4	27.0	52.6
	Replace (w. shared)	0.45B	57.8	52.0	<u>56.7</u>	<u>71.4</u>	23.6	52.3
	<b>LightMoE</b>	0.45B	<b>59.7</b>	<b>55.7</b>	56.3	<b>74.6</b>	30.4	<b>55.3</b>
40%	MC-SMoE*	1.65B	57.0	<u>50.6</u>	40.3	<b>74.5</b>	28.4	<u>50.2</u>
	MoBE	0.45B	37.2	28.6	<b>54.0</b>	65.4	<u>29.9</u>	43.0
	HC-SMoE	0.45B	31.2	33.5	51.5	58.8	16.9	38.4
	MC-SMoE	0.45B	56.0	48.4	50.4	70.8	10.8	47.3
	Replace (w/o shared)	0.45B	56.1	<b>51.3</b>	52.5	65.8	24.7	50.1
	Replace (w. shared)	0.45B	<u>57.7</u>	50.1	<u>53.9</u>	59.0	<u>25.9</u>	49.3
	<b>LightMoE</b>	0.45B	<b>57.9</b>	<b>51.3</b>	53.2	<u>72.6</u>	<b>30.2</b>	<b>53.0</b>
50%	MC-SMoE*	1.65B	50.8	43.8	40.0	<u>73.4</u>	<u>18.5</u>	<u>45.3</u>
	MoBE	0.45B	18.7	9.7	46.4	53.0	<b>21.6</b>	29.9
	HC-SMoE	0.45B	26.2	26.5	47.8	58.0	11.6	34.0
	MC-SMoE	0.45B	50.1	43.1	44.8	67.2	7.2	42.5
	Replace (w/o shared)	0.45B	49.5	<u>46.3</u>	47.1	65.4	13.0	44.3
	Replace (w. shared)	0.45B	<u>51.4</u>	44.5	<b>49.3</b>	56.2	6.7	41.6
	<b>LightMoE</b>	0.45B	<b>56.1</b>	<b>48.4</b>	<u>48.1</u>	<b>74.2</b>	13.5	<b>48.1</b>

with over three times the trainable parameters, MC-SMoE\* still lags behind our method by 2.8%. This demonstrates that our method strikes a superior balance among compression efficiency, training efficiency, and model performance.

For model preservation tasks, our method maintains robust performance even under high compression ratios. Notably, on the Math task, our approach preserves 94% of LoRA’s performance while reducing the model parameters by 50%. This demonstrates that our method can effectively preserve the existing ability of the model. For model adaptation tasks, although performance fluctuates across different specialized tasks and compression ratios, our method outperforms alternative approaches. This indicates that our technique successfully enables model adaptation to an unfamiliar downstream task while simultaneously achieving model compression.

Furthermore, the ‘‘Replace (w/o shared)’’ method achieves performance comparable to MC-SMoE at a 30% ratio and surpasses it at 40%. Notably, even compared to MC-SMoE\*, it maintains comparable performance at both 40% and 50% ratios. This shows that directly replacing less important experts is a strong baseline for compressing MoE models.

Table 2. Comparison of different experts selection methods for LightMoE on the Math and Code tasks. Our adaptive thresholding method can select the most appropriate experts for replacing, adapting to different compression ratios.

Ratio	Selection Methods	Math	Code
		GSM8K	HumanEval
30%	Uniform	58.1	55.1
	Average	<u>59.4</u>	<u>55.5</u>
	<b>Adaptive</b>	<b>59.7</b>	<b>55.7</b>
50%	Uniform	<b>57.1</b>	<u>47.9</u>
	Average	54.6	43.0
	<b>Adaptive</b>	<u>56.1</u>	<b>48.4</b>

Table 3. Comparison of expert grouping strategies for OLMoE on the Math task at different compression ratios.

Ratio	K-means	Dominant (Ours)
30%	<b>60.0</b>	59.7
40%	56.1	<b>57.9</b>
50%	54.9	<b>56.1</b>

### 4.3. Ablation Study

**Impact of expert selection scheme.** To assess the effectiveness of our adaptive thresholding approach, we conduct an ablation study on different expert selection methods: ‘‘Uniform’’ (constant threshold per layer), ‘‘Average’’ (same

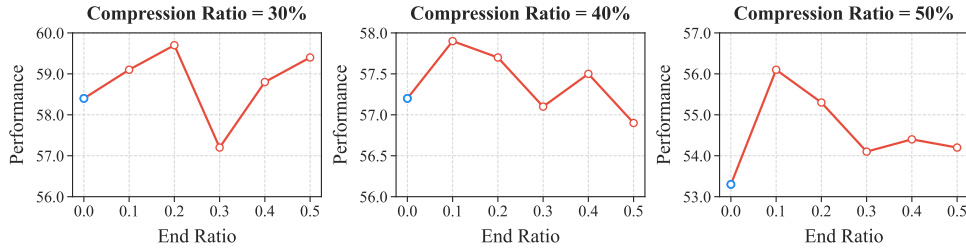


Figure 4. Comparison of different end ratios for LightMoE on the Math task. Directly replacing (blue points) is consistently sub-optimal, which shows the effectiveness of our annealed expert replacement strategy (red points).

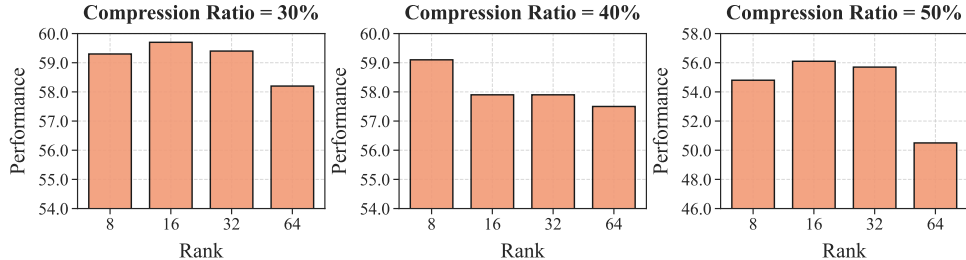


Figure 5. Comparison of different ranks at different compression ratios on the Math task.

number of selected experts per layer), and “Adaptive” (ours). Experimental results are produced on the Math and Code tasks, as shown in Table 2. At a low compression ratio, our method performs comparably to the “Average” selection method but outperforms the “Uniform” selection method. At a high compression ratio, our method performs similarly to the “Uniform” but significantly outperforms the “Average”. This indicates that our method can select the most appropriate experts for replacing, adapting to different compression ratios effectively.

**Impact of expert grouping strategy.** To explore different ways of grouping experts, we compare our method with the K-means clustering strategy, which is adapted from HC-SMoE (Chen et al., 2025a). As shown in Table 3, both strategies perform similarly at a mild 30% ratio. However, as the compression becomes more aggressive, our method demonstrates a clear advantage. At the 40% and 50% ratios, our approach significantly outperforms K-means. We attribute this performance gap to the distinct mechanisms of group formation. Our method focuses on preserving the “dominant” experts and grouping similar experts around them. In contrast, K-means computes average centroids for all experts. When the compression is high, K-means risks inadvertently merging critical experts into a general group, leading to the irreversible loss of expert-specific knowledge. This suggests that explicitly preserving dominant experts is crucial to maintaining performance under high compression.

**Impact of decay ratio.** Figure 4 illustrates how the end ratio hyperparameter affects model performance. Directly replacing (blue points) is consistently sub-optimal, which

shows the effectiveness of our annealed expert replacement strategy. Furthermore, we find that that lower end ratios, specifically 0.1 or 0.2, can often yield the best results.

**Impact of adaptation rank.** To investigate the impact of adaptation rank, we conduct an ablation study across various ranks using the Math task, with results presented in Figure 5. Overall, we observe that lower ranks generally yield superior performance. Specifically, at a 30% compression ratio, performance peaks at rank 16, with a slight drop at higher ranks. Similarly, at 40% and 50% compression ratios, the best performance is achieved at relatively low ranks, while increasing the rank leads to performance degradation. These findings suggest that smaller ranks are generally more effective at higher compression levels.

## 5. Conclusion

In this paper, we introduce a novel expert compression paradigm termed expert replacing. Our empirical findings demonstrate that even a simple baseline of this paradigm yields promising results. Building on this foundation, we propose LightMoE, a framework that enhances the paradigm by introducing adaptive expert selection, hierarchical expert construction, and an annealed recovery strategy. Experimental results across diverse tasks confirm the effectiveness of our approach. LightMoE achieves performance comparable to LoRA fine-tuning at a 30% compression ratio and significantly outperforms existing state-of-the-art methods at a more aggressive 50% ratio. These results indicate that our method successfully reduces the memory footprint of MoE models with minimal training overhead while avoiding

substantial performance degradation. This work not only provides a practical solution for compressing MoE models but also opens up a broader horizon for further research on the expert replacing paradigm. Future work could explore advanced initialization methods and adaptive rank allocation strategies to further unlock the potential of this paradigm.

## References

- Bisk, Y., Zellers, R., Bras, R. L., Gao, J., and Choi, Y. PIQA: reasoning about physical commonsense in natural language. In *AAAI*, pp. 7432–7439. AAAI Press, 2020.
- Chen, I., Liu, H., Sun, W., Chao, C., Hsu, Y., and Lee, C. Retraining-free merging of sparse moe via hierarchical clustering. In *ICML*. OpenReview.net, 2025a.
- Chen, M., Tworek, J., Jun, H., Yuan, Q., de Oliveira Pinto, H. P., Kaplan, J., Edwards, H., Burda, Y., Joseph, N., Brockman, G., Ray, A., Puri, R., Krueger, G., Petrov, M., Khlaaf, H., Sastry, G., Mishkin, P., Chan, B., Gray, S., Ryder, N., Pavlov, M., Power, A., Kaiser, L., Bavarian, M., Winter, C., Tillet, P., Such, F. P., Cummings, D., Plappert, M., Chantzis, F., Barnes, E., Herbert-Voss, A., Guss, W. H., Nichol, A., Paino, A., Tezak, N., Tang, J., Babuschkin, I., Balaji, S., Jain, S., Saunders, W., Hesse, C., Carr, A. N., Leike, J., Achiam, J., Misra, V., Morikawa, E., Radford, A., Knight, M., Brundage, M., Murati, M., Mayer, K., Welinder, P., McGrew, B., Amodei, D., McCandlish, S., Sutskever, I., and Zaremba, W. Evaluating large language models trained on code. *CoRR*, abs/2107.03374, 2021.
- Chen, X., Ha, M., Lan, Z., Zhang, J., and Li, J. Mobe: Mixture-of-basis-experts for compressing moe-based llms. *arXiv preprint arXiv:2508.05257*, 2025b.
- Clark, C., Lee, K., Chang, M., Kwiatkowski, T., Collins, M., and Toutanova, K. Boolq: Exploring the surprising difficulty of natural yes/no questions. In *NAACL-HLT (1)*, pp. 2924–2936. Association for Computational Linguistics, 2019.
- Clark, P., Cowhey, I., Etzioni, O., Khot, T., Sabharwal, A., Schoenick, C., and Tafjord, O. Think you have solved question answering? try arc, the ai2 reasoning challenge. *arXiv preprint arXiv:1803.05457*, 2018.
- Cobbe, K., Kosaraju, V., Bavarian, M., Chen, M., Jun, H., Kaiser, L., Plappert, M., Tworek, J., Hilton, J., Nakano, R., et al. Training verifiers to solve math word problems. *arXiv preprint arXiv:2110.14168*, 2021.
- Dai, D., Dong, L., Ma, S., Zheng, B., Sui, Z., Chang, B., and Wei, F. Stablemoe: Stable routing strategy for mixture of experts. *arXiv preprint arXiv:2204.08396*, 2022.
- Dai, D., Deng, C., Zhao, C., Xu, R. X., Gao, H., Chen, D., Li, J., Zeng, W., Yu, X., Wu, Y., Xie, Z., Li, Y. K., Huang, P., Luo, F., Ruan, C., Sui, Z., and Liang, W. Deepseekmoe: Towards ultimate expert specialization in mixture-of-experts language models. In *ACL (1)*, pp. 1280–1297. Association for Computational Linguistics, 2024.
- Eliseev, A. and Mazur, D. Fast inference of mixture-of-experts language models with offloading. *arXiv preprint arXiv:2312.17238*, 2023.
- Grattafiori, A., Dubey, A., Jauhri, A., Pandey, A., Kadian, A., Al-Dahle, A., Letman, A., Mathur, A., Schelten, A., Vaughan, A., et al. The llama 3 herd of models. *arXiv preprint arXiv:2407.21783*, 2024.
- Han, Z., Gao, C., Liu, J., Zhang, J., and Zhang, S. Q. Parameter-efficient fine-tuning for large models: A comprehensive survey. *arXiv preprint arXiv:2403.14608*, 2024.
- Hayou, S., Ghosh, N., and Yu, B. Lora+: Efficient low rank adaptation of large models. In *ICML*. OpenReview.net, 2024.
- He, Y., Liu, Y., Liang, C., and Awadalla, H. H. Efficiently editing mixture-of-experts models with compressed experts. *arXiv preprint arXiv:2503.00634*, 2025.
- Hu, E. J., Shen, Y., Wallis, P., Allen-Zhu, Z., Li, Y., Wang, S., Wang, L., Chen, W., et al. Lora: Low-rank adaptation of large language models. *ICLR*, 1(2):3, 2022.
- Huang, W., Liao, Y., Liu, J., He, R., Tan, H., Zhang, S., Li, H., Liu, S., and Qi, X. Mc-moe: Mixture compressor for mixture-of-experts llms gains more. *arXiv preprint arXiv:2410.06270*, 2024.
- Iverson, H., Wang, Y., Pyatkin, V., Lambert, N., Peters, M., Dasigi, P., Jang, J., Wadden, D., Smith, N. A., Beltagy, I., and Hajishirzi, H. Camels in a changing climate: Enhancing lm adaptation with tulu 2, 2023.
- Jiang, A. Q., Sablayrolles, A., Roux, A., Mensch, A., Savary, B., Bamford, C., Chaplot, D. S., Casas, D. d. l., Hanna, E. B., Bressand, F., et al. Mixtral of experts. *arXiv preprint arXiv:2401.04088*, 2024.
- Kim, G., Chu, G., and Yang, E. Every expert matters: Towards effective knowledge distillation for mixture-of-experts language models. *arXiv preprint arXiv:2502.12947*, 2025.
- Kim, Y., Lim, H., and Han, D. Scaling beyond the gpu memory limit for large mixture-of-experts model training. In *ICML*. OpenReview.net, 2024.

- Lei, T., Bai, J., Brahma, S., Ainslie, J., Lee, K., Zhou, Y., Du, N., Zhao, V. Y., Wu, Y., Li, B., Zhang, Y., and Chang, M. Conditional adapters: Parameter-efficient transfer learning with fast inference. In *NeurIPS*, 2023.
- Lepikhin, D., Lee, H., Xu, Y., Chen, D., Firat, O., Huang, Y., Krikun, M., Shazeer, N., and Chen, Z. Gshard: Scaling giant models with conditional computation and automatic sharding. *arXiv preprint arXiv:2006.16668*, 2020.
- Lester, B., Al-Rfou, R., and Constant, N. The power of scale for parameter-efficient prompt tuning. *arXiv preprint arXiv:2104.08691*, 2021.
- Li, P., Jin, X., Cheng, Y., and Chen, T. Examining post-training quantization for mixture-of-experts: A benchmark. *arXiv preprint arXiv:2406.08155*, 2024a.
- Li, P., Zhang, Z., Yadav, P., Sung, Y., Cheng, Y., Bansal, M., and Chen, T. Merge, then compress: Demystify efficient smoe with hints from its routing policy. In *ICLR*. OpenReview.net, 2024b.
- Li, X. L. and Liang, P. Prefix-tuning: Optimizing continuous prompts for generation. *arXiv preprint arXiv:2101.00190*, 2021.
- Liu, A., Feng, B., Wang, B., Wang, B., Liu, B., Zhao, C., Deng, C., Ruan, C., Dai, D., Guo, D., et al. Deepseek-v2: A strong, economical, and efficient mixture-of-experts language model. *arXiv preprint arXiv:2405.04434*, 2024a.
- Liu, B., Ding, L., Shen, L., Peng, K., Cao, Y., Cheng, D., and Tao, D. Diversifying the mixture-of-experts representation for language models with orthogonal optimizer. In *ECAI*, volume 392 of *Frontiers in Artificial Intelligence and Applications*, pp. 2966–2973. IOS Press, 2024b.
- Liu, E., Zhu, J., Lin, Z., Ning, X., Blaschko, M. B., Yan, S., Dai, G., Yang, H., and Wang, Y. Efficient expert pruning for sparse mixture-of-experts language models: Enhancing performance and reducing inference costs. *arXiv preprint arXiv:2407.00945*, 2024c.
- Liu, S., Wang, C., Yin, H., Molchanov, P., Wang, Y. F., Cheng, K., and Chen, M. Dora: Weight-decomposed low-rank adaptation. In *ICML*. OpenReview.net, 2024d.
- Loshchilov, I. and Hutter, F. Decoupled weight decay regularization. In *ICLR (Poster)*. OpenReview.net, 2019.
- Lu, X., Liu, Q., Xu, Y., Zhou, A., Huang, S., Zhang, B., Yan, J., and Li, H. Not all experts are equal: Efficient expert pruning and skipping for mixture-of-experts large language models. *arXiv preprint arXiv:2402.14800*, 2024.
- Meng, F., Wang, Z., and Zhang, M. Pissa: Principal singular values and singular vectors adaptation of large language models. In *NeurIPS*, 2024.
- Muennighoff, N., Soldaini, L., Groeneveld, D., Lo, K., Morrison, J., Min, S., Shi, W., Walsh, E. P., Tafjord, O., Lambert, N., Gu, Y., Arora, S., Bhagia, A., Schwenk, D., Wadden, D., Wettig, A., Hui, B., Dettmers, T., Kiela, D., Farhadi, A., and et al. Olmoe: Open mixture-of-experts language models. In *ICLR*. OpenReview.net, 2025.
- Rücklé, A., Geigle, G., Glockner, M., Beck, T., Pfeiffer, J., Reimers, N., and Gurevych, I. Adapterdrop: On the efficiency of adapters in transformers. In *EMNLP (1)*, pp. 7930–7946. Association for Computational Linguistics, 2021.
- Sakaguchi, K., Bras, R. L., Bhagavatula, C., and Choi, Y. Winogrande: an adversarial winograd schema challenge at scale. *Commun. ACM*, 64(9):99–106, 2021.
- Shen, Y., Guo, Z., Cai, T., and Qin, Z. Jetmoe: Reaching llama2 performance with 0.1 m dollars. *arXiv preprint arXiv:2404.07413*, 2024.
- Song, Z., Huang, S., Wu, Y., and Kang, Z. Layer importance and hallucination analysis in large language models via enhanced activation variance-sparsity. *arXiv preprint arXiv:2411.10069*, 2024.
- Taori, R., Gulrajani, I., Zhang, T., Dubois, Y., Li, X., Guestrin, C., Liang, P., and Hashimoto, T. B. Stanford alpaca: An instruction-following llama model. [https://github.com/tatsu-lab/stanford\\_alpaca](https://github.com/tatsu-lab/stanford_alpaca), 2023.
- Touvron, H., Martin, L., Stone, K., Albert, P., Almahairi, A., Babaei, Y., Bashlykov, N., Batra, S., Bhargava, P., Bhosale, S., et al. Llama 2: Open foundation and fine-tuned chat models. *arXiv preprint arXiv:2307.09288*, 2023.
- Wang, Y., Mukherjee, S., Liu, X., Gao, J., Awadallah, A. H., and Gao, J. Adamix: Mixture-of-adapters for parameter-efficient tuning of large language models. *arXiv preprint arXiv:2205.12410*, 1(2):4, 2022.
- Wang, Y., Ivison, H., Dasigi, P., Hessel, J., Khot, T., Chandu, K. R., Wadden, D., MacMillan, K., Smith, N. A., Beltagy, I., and Hajishirzi, H. How far can camels go? exploring the state of instruction tuning on open resources, 2023a.
- Wang, Z., Panda, R., Karlinsky, L., Feris, R., Sun, H., and Kim, Y. Multitask prompt tuning enables parameter-efficient transfer learning. *arXiv preprint arXiv:2303.02861*, 2023b.

- Wang, Z., Chen, D., Dai, D., Xu, R., Li, Z., and Wu, Y. Let the expert stick to his last: Expert-specialized fine-tuning for sparse architectural large language models. In *EMNLP*, pp. 784–801. Association for Computational Linguistics, 2024.
- Wu, X., Huang, S., and Wei, F. Mixture of lora experts. *arXiv preprint arXiv:2404.13628*, 2024.
- Xie, Y., Zhang, Z., Zhou, D., Xie, C., Song, Z., Liu, X., Wang, Y., Lin, X., and Xu, A. Moe-pruner: Pruning mixture-of-experts large language model using the hints from its router. *arXiv preprint arXiv:2410.12013*, 2024.
- Xu, H., Liu, H., Gong, W., Deng, X., and Wang, H. Sparse mixture of experts language models excel in knowledge distillation. In *CCF International Conference on Natural Language Processing and Chinese Computing*, pp. 80–91. Springer, 2024.
- Xu, L., Xie, H., Qin, S.-Z. J., Tao, X., and Wang, F. L. Parameter-efficient fine-tuning methods for pretrained language models: A critical review and assessment. *arXiv preprint arXiv:2312.12148*, 2023.
- Yang, A., Yang, B., Hui, B., Zheng, B., Yu, B., Zhou, C., Li, C., Li, C., Liu, D., Huang, F., Dong, G., Wei, H., Lin, H., Tang, J., Wang, J., Yang, J., Tu, J., Zhang, J., Ma, J., Xu, J., Zhou, J., Bai, J., He, J., Lin, J., Dang, K., Lu, K., Chen, K., Yang, K., Li, M., Xue, M., Ni, N., Zhang, P., Wang, P., Peng, R., Men, R., Gao, R., Lin, R., Wang, S., Bai, S., Tan, S., Zhu, T., Li, T., Liu, T., Ge, W., Deng, X., Zhou, X., Ren, X., Zhang, X., Wei, X., Ren, X., Fan, Y., Yao, Y., Zhang, Y., Wan, Y., Chu, Y., Liu, Y., Cui, Z., Zhang, Z., and Fan, Z. Qwen2 technical report. *arXiv preprint arXiv:2407.10671*, 2024a.
- Yang, A., Yang, B., Zhang, B., Hui, B., Zheng, B., Yu, B., Li, C., Liu, D., Huang, F., Wei, H., Lin, H., Yang, J., Tu, J., Zhang, J., Yang, J., Yang, J., Zhou, J., Lin, J., Dang, K., Lu, K., Bao, K., Yang, K., Yu, L., Li, M., Xue, M., Zhang, P., Zhu, Q., Men, R., Lin, R., Li, T., Xia, T., Ren, X., Ren, X., Fan, Y., Su, Y., Zhang, Y., Wan, Y., Liu, Y., Cui, Z., Zhang, Z., and Qiu, Z. Qwen2.5 technical report. *arXiv preprint arXiv:2412.15115*, 2024b.
- Yang, C., Sui, Y., Xiao, J., Huang, L., Gong, Y., Duan, Y., Jia, W., Yin, M., Cheng, Y., and Yuan, B. Moe-i2: Compressing mixture of experts models through inter-expert pruning and intra-expert low-rank decomposition. *arXiv preprint arXiv:2411.01016*, 2024c.
- Yu, H., Cui, X., Zhang, H., and Wang, H. fMoE: Fine-grained expert offloading for large mixture-of-experts serving. *arXiv preprint arXiv:2502.05370*, 2025.
- Yu, L., Jiang, W., Shi, H., Yu, J., Liu, Z., Zhang, Y., Kwok, J. T., Li, Z., Weller, A., and Liu, W. Metamath: Bootstrap your own mathematical questions for large language models. In *ICLR*. OpenReview.net, 2024.
- Zhang, S., Frey, B., and Bansal, M. Chren: Cherokee-english machine translation for endangered language revitalization. In *EMNLP (1)*, pp. 577–595. Association for Computational Linguistics, 2020.
- Zheng, T., Zhang, G., Shen, T., Liu, X., Lin, B. Y., Fu, J., Chen, W., and Yue, X. Opencodeinterpreter: Integrating code generation with execution and refinement. In *ACL (Findings)*, pp. 12834–12859. Association for Computational Linguistics, 2024.

## A. Supplemental Experimental Results

### A.1. Results on DeepSeek Model

To further verify the effectiveness of LightMoE, we extend our evaluation to the DeepSeek-V2-Lite model (Liu et al., 2024a), with 15.7B total and 2.4B active parameters. With the exception of the first layer, this model natively consists of 64 routed experts and 2 shared experts per layer. We maintain the same experimental setup and training configurations as those used for the OLMoE model to ensure consistency. The performance comparison across diverse tasks and compression ratios is presented in Table 4.

Overall, LightMoE demonstrates robust performance, achieving the best or second-best scores across most tasks. This advantage becomes particularly pronounced at higher compression ratios. While MoBE performs slightly better at a mild 30% compression ratio, it suffers from a drastic performance collapse as compression increases, dropping to an average of 38.6% at the 50% ratio. In contrast, LightMoE maintains superior stability, securing the highest average performance at both 40% and 50% ratios. This highlights the robustness of our approach under aggressive compression constraints.

A critical observation in Table 4 is the performance on the Math task. Notably, LightMoE (33.3%) lags behind the standard LoRA baseline (38.9%), while other compression methods like MoBE (54.3%) and MC-SMoE (48.4%) significantly outperform LoRA. We attribute this anomaly primarily to the rank capacity. Under the constraint of equal trainable parameters, LightMoE operates with a rank of 16, whereas LoRA uses a rank of 54, and other baselines utilize ranks exceeding 80. This trend suggests that complex mathematical reasoning is highly sensitive to low-rank bottlenecks. While our design ensures overall stability, the reduced rank limits the specific capacity for the math task in DeepSeek model. Future work could address this trade-off by exploring adaptive rank allocation strategies.

### A.2. Impact of Sample size on Importance Scoring

To evaluate the amount of data needed to select the less important experts for a task, we assess the model’s performance on the Math task using varying token counts, ranging from  $2^{13}$  to  $2^{19}$ . As shown in Table 5, we observe that the performance improves as the number of tokens increases from  $2^{13}$  to  $2^{17}$ , highlighting the necessity of adequate data for accurate expert selection. However, performance gains saturate as the sample size reaches  $2^{17}$ . Specifically, increasing the sample size from  $2^{17}$  to  $2^{19}$  yields minimal gains across all compression ratios. This indicates that the sample size of  $2^{17}$  is sufficiently large to identify the less important experts.

### A.3. Sensitivity Analysis of Adaptive Thresholding Hyperparameters

To provide a systematic justification for the hyperparameter choice in our adaptive thresholding mechanism, we introduce a parameter  $\max\Delta$  to control the bounds of the layer-specific thresholds. Specifically, the minimum and maximum thresholds are defined as:

$$p_{\min} = (1 - \max\Delta)\hat{p}, \quad p_{\max} = (1 + \max\Delta)\hat{p}. \quad (8)$$

We evaluate the model performance on the Math task with  $\max\Delta \in \{0, 0.1, 0.15, 0.2, 0.25, 0.3, \infty\}$ . Notably,  $\max\Delta = 0$  is equivalent to the "Uniform" strategy, while  $\max\Delta = \infty$  removes the clipping bounds entirely.

The results presented in Table 6 highlight two key observations. First, at a moderate 30% compression ratio, our adaptive approach significantly outperforms the uniform baseline. Introducing a reasonable clipping range improves performance from 58.1% to 59.7%, confirming the benefit of varying thresholds based on layer importance. Second, the results demonstrate that moderate clipping is essential. Removing the bounds entirely leads to performance degradation compared to the optimal range (e.g., dropping from 59.7% to 58.6% at the 30% ratio). This suggests that while flexibility is beneficial, preventing the thresholds from becoming too extreme is necessary for stability.

In conclusion, values between 0.15 and 0.2 consistently yield robust performance across different compression ratios. This validates our default choice of  $\max\Delta = 0.2$  as a systematic and effective setting that balances adaptivity with numerical stability.

### A.4. Impact of Group Size

We explore the impact of incrementally increasing the group size of LightMoE from 1 to 4. Figure 6 illustrates performance across various group sizes and compression ratios on the Math task. At a mild 30% compression ratio, the performance of all group sizes vary by less than 0.9%, showing that multiple shared bases has little effect when ample parameters remain.

In contrast, as compression becomes more aggressive, the benefit of larger group sizes becomes pronounced. In particular, at a 50% compression ratio, performance improves with increasing group size. This trend suggests that under constrained parameter budgets, constructing multiple shared bases by grouping is crucial for preserving the model’s knowledge and capabilities.

### A.5. Exploration of Annealing Schedules

To investigate the impact of the annealing schedule on model performance, we compare our default linear decay strategy against an exponential decay strategy. While the linear

Table 4. Performance comparison on DeepSeek model across methods and tasks at different compression ratios.

Ratio	Methods	# Params	Math	Code	Common.	Specialized Tasks		Average
			GSM8K	HumanEval	8 Sub-Tasks	Intent	Translation	
0%	Original	-	3.0	53.9	61.8	0.0	12.2	26.2
0%	LoRA	0.96B	38.9	58.0	62.3	81.0	19.9	52.0
30%	MoBE	0.96B	<b>54.3</b>	47.7	<b>59.7</b>	<u>80.2</u>	<b>27.0</b>	<b>53.8</b>
	HC-SMoE	0.96B	36.8	51.6	57.8	75.8	<u>26.9</u>	49.8
	MC-SMoE	0.96B	<u>48.4</u>	<u>53.7</u>	57.0	60.6	26.8	49.3
	<b>LightMoE</b>	0.96B	33.3	<b>58.1</b>	<u>59.2</u>	<b>81.2</b>	25.3	<u>51.4</u>
40%	MoBE	0.96B	<b>50.9</b>	40.6	<b>57.6</b>	71.2	24.5	<u>49.0</u>
	HC-SMoE	0.96B	43.0	47.8	55.1	<u>72.2</u>	26.5	48.9
	MC-SMoE	0.96B	<u>47.6</u>	<u>50.2</u>	54.7	61.8	<u>27.5</u>	48.4
	<b>LightMoE</b>	0.96B	33.7	<b>55.8</b>	<u>57.3</u>	<b>80.0</b>	<b>27.7</b>	<b>50.9</b>
50%	MoBE	0.96B	<u>39.3</u>	19.2	50.7	63.8	19.9	38.6
	HC-SMoE	0.96B	34.3	<u>43.5</u>	<u>53.0</u>	<u>72.4</u>	<b>25.8</b>	<u>45.8</u>
	MC-SMoE	0.96B	<b>42.2</b>	38.2	51.3	47.6	22.9	40.4
	<b>LightMoE</b>	0.96B	32.8	<b>51.5</b>	<b>54.3</b>	<b>79.4</b>	<u>24.0</u>	<b>48.4</b>

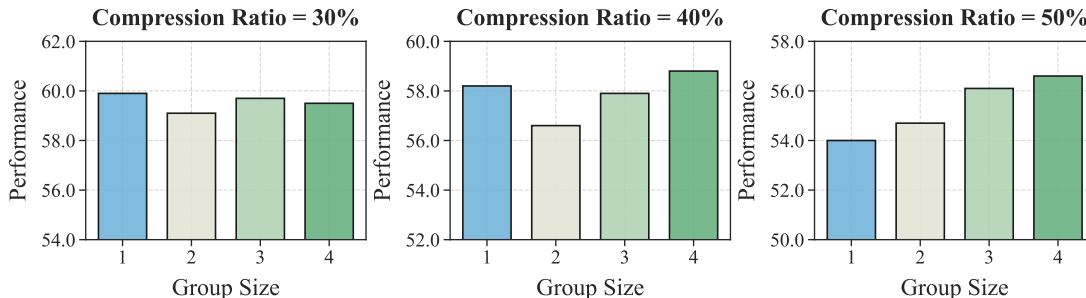


Figure 6. Comparison of different group sizes at different compression ratios for OLMoE on the Math task.

Table 5. Ablation study on the impact of sample size on OLMoE performance.

Ratio	Number of Tokens			
	2 <sup>13</sup>	2 <sup>15</sup>	2 <sup>17</sup>	2 <sup>19</sup>
30%	57.4	59.1	<b>59.7</b>	59.6
40%	55.1	56.6	<u>57.9</u>	<b>58.4</b>
50%	53.9	54.5	<u>56.1</u>	<b>56.3</b>

Table 6. Sensitivity analysis of the clipping range parameter maxΔ for OLMoE on the Math task.

Ratio	Clipping Range max Δ						
	0	0.1	0.15	0.2	0.25	0.3	∞
30%	58.1	59.4	<b>59.7</b>	<b>59.7</b>	59.3	58.6	58.6
50%	<b>57.1</b>	55.6	55.8	<u>56.1</u>	54.1	54.3	54.3

strategy decreases  $\beta$  at a constant rate, the exponential strategy introduces a curvature controlled by a hyperparameter  $\gamma$ . Formally, maintaining consistency with the notation in Section 3.3, the annealing factor  $\beta$  under the exponential schedule is defined as:

$$\beta = \max\left(\frac{e^{-\gamma\tau} - e^{-\gamma}}{1 - e^{-\gamma}}, 0\right), \quad \text{where } \tau = \frac{t}{\epsilon T}. \quad (9)$$

Here,  $\tau$  represents the normalized training progress relative to the annealing period, and  $\gamma$  modulates the decay shape. A larger  $\gamma$  causes  $\beta$  to drop more rapidly initially, whereas a smaller  $\gamma$  maintains a higher value for a longer duration. Visualizations of these decay trajectories are provided in Figure 7.

We evaluate this strategy with  $\gamma$  values of 1.0, 3.0, and 5.0. The results on the Math task are summarized in Table 7.

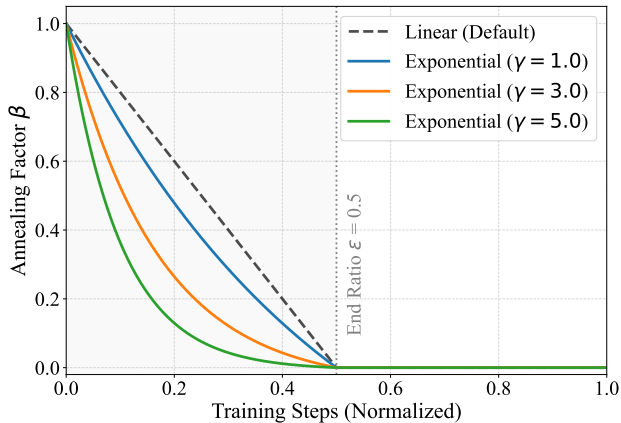


Figure 7. Comparison of different annealing schedules. The dashed line represents the linear decay strategy, while solid lines depict exponential decay strategies with varying  $\gamma$ . All schedules converge to zero at the end ratio  $\epsilon$ .

Table 7. Comparison of linear and exponential annealing schedules for OLMoE on the Math task.

Ratio	Linear	Exponential Decay		
		$\gamma = 1.0$	$\gamma = 3.0$	$\gamma = 5.0$
30%	<u>59.7</u>	<b>59.8</b>	59.6	58.7
40%	57.9	56.1	<u>58.2</u>	<b>58.4</b>
50%	<b>56.1</b>	54.5	54.4	<u>56.0</u>

Overall, the performance differences between the linear and exponential schedules are marginal. However, the linear schedule demonstrates remarkable robustness across different compression levels. It achieves the best performance at the aggressive 50% compression ratio and ranks second-best at the 30% ratio. Even at 40%, where it falls slightly behind the exponential setting, the gap is negligible.

In contrast, the exponential strategy proves sensitive to the hyperparameter  $\gamma$ . A lower  $\gamma$  performs well at low compression but degrades at high compression, whereas a higher  $\gamma$  shows the opposite trend. No single  $\gamma$  value yields optimal results across all scenarios. Consequently, we adopt the Linear schedule as a simple yet sufficiently effective solution, as it delivers consistently high performance without the need for additional hyperparameter tuning.

### B. Efficiency Analysis

To assess the inference efficiency of our approach, we evaluate the model across four key metrics: total parameter count, GPU memory usage, MoE average active parameters per token, and inference latency. The results for the OLMoE model on the Math task are summarized in Table 8.

As the compression ratio increases, we observe a substantial reduction in memory requirements. Specifically, the mem-

Table 8. Inference efficiency comparison on the Math task under different compression ratios.

Ratio	Total Params	Memory Usage	MoE Active Params	Latency (ms/token)
0%	6.92 B	12.89 GB	0.81 B	8.09
30%	4.82 B	9.09 GB	0.77 B	8.71
40%	4.14 B	7.85 GB	0.73 B	8.32
50%	3.47 B	6.63 GB	0.70 B	8.01

ory footprint decreases by nearly half, dropping from 12.89 GB in the original model to 6.63 GB at the 50% compression ratio. In terms of computational cost, the decrease in the number of parameters activated within the MoE layers is less pronounced. This is expected, as our method primarily targets and compresses redundant experts that are less frequently activated, while preserving the critical experts that contribute most to the active parameter count. Moreover, although replacing experts with shared bases and adapters introduces slight architectural complexity, our method maintains an inference latency comparable to the original model. These findings demonstrate that LightMoE effectively reduces parameter redundancy and memory usage without compromising inference efficiency.

### C. Training Dynamics Analysis

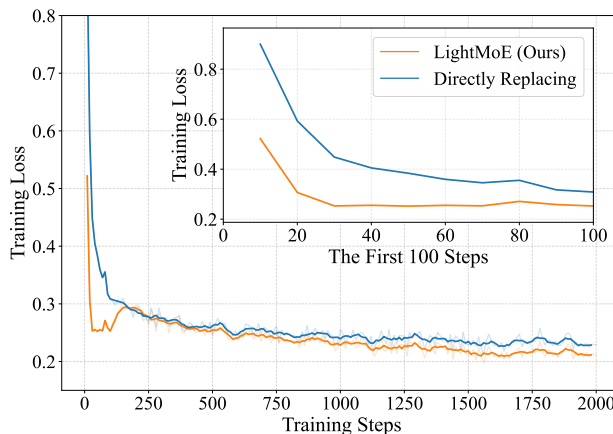


Figure 8. Training loss trajectories of LightMoE versus the Directly Replacing baseline on the Math task with OLMoE at a 50% compression ratio.

To validate the intuition behind our annealing strategy, we visualize the training dynamics of LightMoE compared to the Directly Replacing baseline in Figure 8.

As illustrated in the inset of Figure 8, the Directly Replacing baseline suffers from a severe optimization instability, evidenced by a sharp initial spike in loss. This indicates that the abrupt parameter substitution destabilizes the model,

forcing the optimization trajectory to recover from a high-loss, sub-optimal state. In contrast, LightMoE ensures a smooth start with minimal loss, effectively mitigating the destructive initial shock.

As training progresses and  $\beta$  decays, LightMoE exhibits a slight rise in loss. This phenomenon represents the critical transfer of capabilities from the original experts to the compressed modules. Effectively, the annealing phase acts as a warm-up period, allowing the compressed modules to implicitly align with the original experts’ behavior.

Crucially, despite this transient rise, the loss trajectory of LightMoE remains lower than that of the baseline throughout the training process. This suggests that the smooth transition keeps the model in a better region of the parameter space, avoiding the suboptimal local minima that the baseline falls into.

Moreover, although our current strategy is effective, the temporary rise in loss implies a brief gap in capability during the transition. Future work could explore more adaptive schedules and better initialization methods to further mitigate this fluctuation, thereby enhancing the training stability of the expert replacing paradigm.

### D. Base Threshold Settings

Table 9. Base threshold  $\hat{p}$  settings calibrated for OLMoE and DeepSeek models. The average number of selected experts per layer (Avg # Exp.) corresponds to the target compression ratio.

Ratio (%)	Avg # Exp.	Base Threshold $\hat{p}$				
		Math	Code	Common.	Intent	Trans.
<i>Model: OLMoE-1B-7B-SFT</i>						
30	≈ 24	0.110	0.095	0.185	0.055	0.036
40	≈ 31	0.180	0.159	0.275	0.098	0.059
50	≈ 38	0.268	0.240	0.382	0.168	0.092
<i>Model: DeepSeek-V2-Lite</i>						
30	≈ 26	0.160	0.200	0.192	0.085	0.058
40	≈ 33	0.240	0.285	0.280	0.142	0.098
50	≈ 40	0.330	0.385	0.380	0.215	0.146

To facilitate reproducibility, we provide the specific hyperparameter configurations used to achieve the target compression ratios for both the OLMoE and DeepSeek models. In the LightMoE framework, the global compression ratio is controlled by the base threshold  $\hat{p}$  defined in Equation (3). This threshold determines the subset of experts selected for replacement. A higher  $\hat{p}$  results in more experts being replaced, thereby increasing the compression ratio.

Since the distribution of expert importance scores varies across domains, the base threshold required to select these

experts differs. Therefore, for each task and target compression ratio, we determine the optimal  $\hat{p}$  via a binary search process on the calibration dataset. Table 9 presents these  $\hat{p}$  values for the five evaluated tasks, alongside the corresponding average number of experts selected per layer.

A distinct pattern emerges from the results. For preservation tasks, including Math, Code, and Commonsense Reasoning, the base thresholds are relatively high. This suggests that in these domains, even the less critical experts selected for replacement retain a moderate level of activation and contribution. Conversely, for adaptation tasks like Intent Recognition and Translation, the thresholds are significantly lower. This indicates that the expert activation in these specialized downstream tasks is highly sparse, allowing a large number of redundant experts to be identified even with a very low threshold.